Fusion Engineering and Design 202 (2024) 114375

Contents lists available at ScienceDirect

Fusion Engineering and Design

journal homepage: www.elsevier.com/locate/fusengdes

Assessment of the relevancy of ENEA Water Loop facility with respect to ITER WCLL TBS Water Cooling System by considering their thermal-hydraulic performances

B. Gonfiotti [a,*], C. Ciurluini [b], F. Giannetti [b], P. Arena [a], A. Del Nevo [a]

[a] ENEA, Department of Fusion and Nuclear Safety Technology, 40032 Camugnano (BO), Italy
[b] DIAEE Department, Sapienza University of Rome, 00186 Roma, Italy

ARTICLE INFO

Keywords:
Water Loop
WCLL-WCS
RELAP5
Normal operational state
LOFA

ABSTRACT

The Water-Cooled Lead-Lithium (WCLL) is one of the two candidate concepts for the Breeding Blanket (BB) of DEMO. A Test Blanket Module (TBM) together with its Water Cooling System (WCS) is going to be installed and tested in the ITER reactor. The WCS acts as primary cooling circuit of the TBM module, and it is designed to reproduce the water thermodynamic conditions expected at the DEMO BB inlet.

During last years, ENEA and the DIAEE of Sapienza University of Rome have carried out the conceptualization of the Water Loop (WL) facility, belonging to the W-HYDRA experimental platform planned at C.R. Brasimone. The W-HYDRA platform is composed by three individual facilities called: Water Loop, Steam, and LIFUS5/Mod4. Water Loop replicates the salient thermal-hydraulic features of the ITER WCLL WCS, and it is equipped with a test section placed inside a Vacuum Vessel (VV) to investigate mock-ups of the whole TBM or its individual parts.

This paper assesses the relevancy of the WL facility with respect to ITER WCLL TBM System comparing their thermal-hydraulic performances during selected operational and accidental conditions. Two RELAP5/Mod3.3 models were developed, and the outcomes of the simulations showed a good agreement, thus demonstrating the effectiveness of WL facility to support the ITER TBM program.

1. Introduction

As part of the efforts in the development of a fusion reactor, the investigation of different Breeding Blanket (BB) concepts is one of the most challenging tasks [1]. Two concepts are currently under investigation: the Water-Cooled Lead-Lithium (WCLL) and the Helium Cooled Pebble Bed (HCPB) [2,3]. A test field for both concepts is the European Test Blanket Module (TBM) program that focuses on the installation of ad-hoc Test Blanket Systems (TBS) in the ITER reactor [4].

In recent years ENEA and its related partners started the conceptualization, design, and construction of the W-HYDRA experimental platform. This platform is composed by three facilities: Water Loop (WL), STEAM, and LIFUS5/Mod4 each devoted to the investigation of the main phenomena occurring in the WCLL-TBS and WCLL-BB systems [5].

WL is a medium-scale facility intended to be a thermal-hydraulic replica of the ITER WCLL Water Cooling System (WCS) [5]. The facility is coupled with a vacuum chamber to test mock-ups up to the size of the WCLL-TBM. These characteristics make WL a perfect test bed for the components to be installed in the WCLL-WCS, and the procedures and phenomena to be investigated in this system.

The present paper describes recent efforts devoted to the analysis of the consistency between the ITER WCLL-WCS and the WL designs. After an initial comparison from the geometrical point of view, thermal-hydraulic analyses are carried out with RELAP5/Mod3.3. These analyses cover both the pulsed normal operational state at end of life, and the response under a loss of flow accident affecting the WCLL-WCS/WL secondary loop.

2. ITER WCLL WCS

The ITER WCLL-WCS transfers the heat deposited in the TBM to the CCWS (Component Cooling Water System). The system consists of three loops: the Primary Loop (PL), an intermediate/Secondary Loop (SL), and the CCWS. A detailed description of the system is provided in [6].

The primary loop is an eight-shaped circuit operating with water at

* Corresponding author.
E-mail address: bruno.gonfiotti@enea.it (B. Gonfiotti).

https://doi.org/10.1016/j.fusengdes.2024.114375
Received 28 September 2023; Received in revised form 15 January 2024; Accepted 18 March 2024
Available online 21 March 2024

15.5 MPa and 111 – 328 °C (295 °C – 328 °C across the TBM). A total mass flow rate of 3.74 kg/s is sufficient to remove the thermal power (about 700 kW) faced by the TBM first wall and breeding zone.

The circuit spans a height of about 25 m: the lowest point is represented by the TBM installed in the vacuum vessel, while the highest point is represented by the piping connecting the heat exchangers placed within the Tokamak Cooling Water System (TCWS) vault. The main components of the primary loop are:

- TA-0006 and TA-0007 delay tanks, slowing down the coolant exiting the TBM to reduce the N^{16}/N^{17} content within the primary coolant before it reaches the TCWS vault.
- HX-0001 hairpin economizer to reduce the temperature of the coolant approaching the HX-0002 heat exchanger while increasing the temperature of the coolant entering the TBM. The hot coolant from the TBM crosses the tube bundle, while the cold water from HX-0002 the shell side.
- HX-0002 hairpin heat exchanger to transfer thermal power from the PL to the SL. The coolant of the primary loop crosses the tube bundle, while the shell side is crossed by the secondary loop coolant.
- A filter and two centrifugal pumps to move the coolant.
- HT-0001 electrical heater to increase the coolant temperature to 295 °C, i.e. the inlet temperature required by the TBM.
- A pressurizer equipped with an electrical heater and a spray system to control the circuit pressure. The component is also connected to a relief tank by means of a Pilot Operated Relief Valve (PORV) and a Safety Relief Valve (SRV).
- A cylindrical Pressure Relief Tank (PRT) to condensate the steam coming from the pressurizer. The relief tank is partially filled with water and the incoming steam is released inside the water column.

The secondary loop is an intermediate circuit preventing the ingress of radioactive substances in the CCWS in case of leakage. The circuit operates with water at 2 MPa and 65 – 105 °C. The loop spans only 3.5 m in height being entirely installed in the TCWS vault. The loop consists of two hairpin heat exchangers (HX-0002 and HX-0003), a filter, a pump, and a pressurizer. The coolant crosses HX-0002 on the shell side, and HX-0003 on the tube side. The pump provides the required mass flow rate (4.3 kg/s), and the pressurizer controls the pressure in the circuit with an electrical heater and a spray system. The pressurizer is also equipped with a PORV and SRV to discharge steam into the same relief tank used also by PL. The PORV and the SRV open at 2.2 and 2.4 MPa, respectively. The closing set-point is set to 2.07 MPa for both valves.

Fig. 1 presents an overview of the main components installed in the TCWS vault. The delay tanks are not shown being installed in the vicinity of TBM and in the vertical shaft (the corridor connecting the vacuum vessel with the TCWS vault). Table 1 summarizes the design (d) and operative (o) conditions of the three loops composing the WCS.

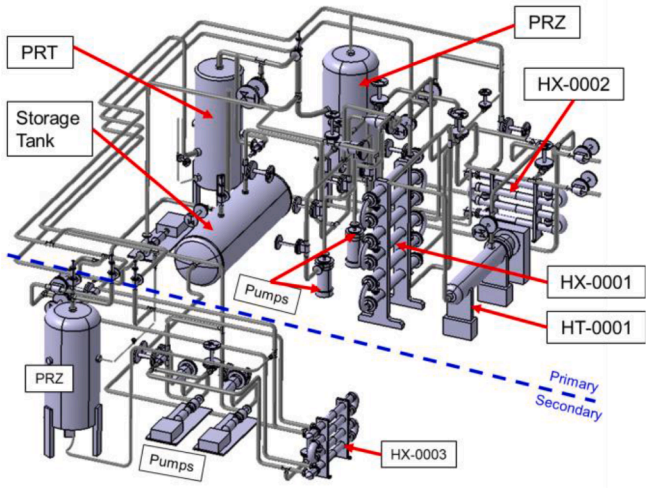

Fig. 1. WCS equipment installed in TCWS Vault [6].

3. ENEA Water Loop (WL)

The ENEA WL facility is a medium-scale integral test facility replicating the salient thermal-hydraulic features of ITER WCLL-WCS [5]. The aim of the facility is to test components, mock-ups, and operative procedures in view of ITER operations. The facility will investigate the WCS in normal and off-normal operative conditions. WL is coupled with a vacuum chamber to allow the testing of mock-ups up to the size of the TBM. The chamber is equipped with an electron beam gun to reproduce the plasma heating of the ITER reactor [5].

Given the aim of the facility, components similar to that of the ITER WCLL-WCS are also adopted for WL. Notable differences between the two facilities are the pipeline disposition due to different space constraints, and the insulation material (MICROTHERM MPS in ITER and PAROC Pro Lamella Mat 80 AluCoat in WL). Fig. 2 shows the disposition of the experimental facility.

4. Geometrical comparison

The first analysis carried out for the ITER WCLL-WCS and WL facility is a geometrical comparison. The aim is to demonstrate that the two facilities have a similar pipeline length and a comparable absolute height of the component's barycenter. The comparison has been done starting from the data adopted in the RELAP5/Mod3.3 WCS and WL input decks employed for the transient analysis described in the next section. The starting point (length = 0 m) is assumed to be at TBM outlet, and the ending point at TBM inlet (the TBM is not considered in this analysis). A preliminary assessment of the characteristics of the two input decks against the relevant CAD has also been done showing the correctness of the two input decks.

As it can be seen in Fig. 3, the barycenter of the main components along the primary loop in WL is at the same height of the WCLL-WCS ones. Delay tank TA-0006 is close to the TBM at the lowest height, and delay tank TA-0007 is in the vertical shaft connecting the Vacuum Vessel Hall with the TCWS vault. The heat exchangers (HX-0001 and HX-0002) and the electrical heater (HT-0001) are also at a similar height in the TCWS vault (about 23 m above the lowest point).

Although, the WL pipeline is about 10% shorter than the WCLL-WCS one (215 m vs 238 m). Local differences also exist in the repartition between pipelines in the surrounding of the TBM and in the TCWS vault.

The secondary loop presents more striking differences (Fig. 4). These differences are also visible in the component's disposition shown in Figs. 1 and 2. The starting and the ending points are assumed to be at the inlet of HX-0002. The height span of the WL circuit is about 1.5 m instead of 3.5 m of the WCLL-WCS. The absolute height of the main components (heat exchangers and pump stage) is quite well reproduced, even if the heat exchangers adopted in WL span a height of 1 m instead of 1.5 m. This deviation is associated with the different 180° curves used to connect the straight segments of the hairpin heat exchangers. However, the curves do not take part to the thermal length of the component, thus do not affect the heat transfer performances. In addition, their

Table 1
WCS design (d) and operative (o) conditions.

Data	Prim.	Second.	CCWS
Pressure (MPa) (d)	18.6	2.4	2.4
Temperature (°C) (d)	360	222	222
Pressure (MPa) (o)	15.5	2.0	<0.6
Temperature (K) (o)	328–110	105–65	31–41
Pump head (m) (o)	83	15	6
Flow Rate (kg/s) (o)	3.74	4.3	17.3

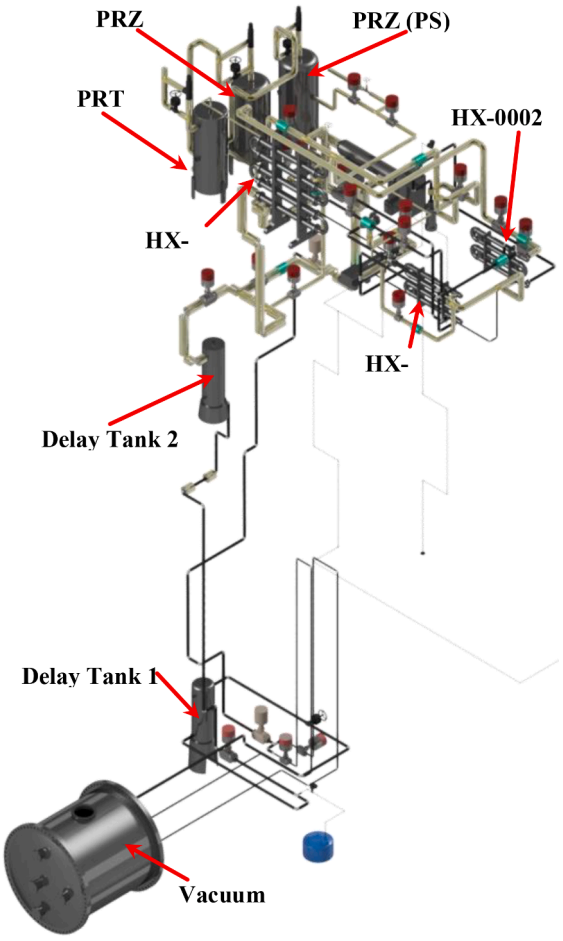

Fig. 2. ENEA Water Loop facility.

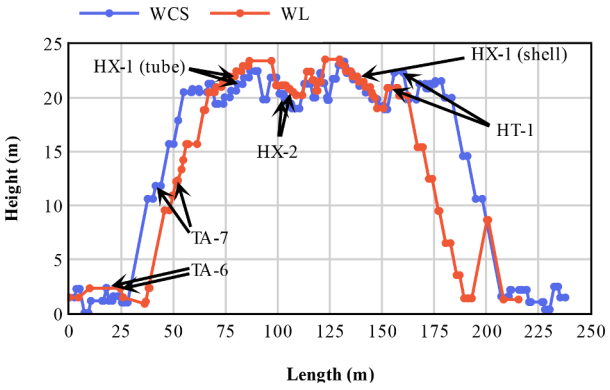

Fig. 3. Length vs height - primary loop.

impact on the loop overall pressure drops is negligible.

Although, the most relevant difference is in the pipeline position and length. In the WCLL-WCS the two heat exchangers are placed in two different areas of the TCWS vault, while they are near in WL. This leads to a total pipeline length difference of 49 m (90 m in WCS and 41 m in WL), and a difference of the total height span of about 2 m (3.5 m in the WCLL-WCS and 1.5 m in WL).

5. Normal operational state at end-of-life

The ITER reactor is characterized by a pulsed normal operation state divided into 4 phases:

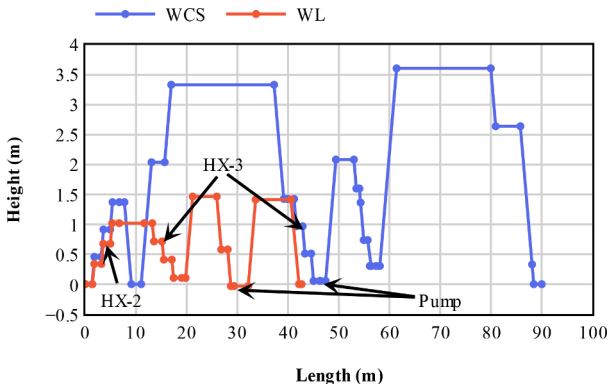

Fig. 4. Length vs height - secondary loop.

- 60 s of ramp-up from zero to full plasma power.
- 450 s of full plasma power ("flat top") providing about 723 kW to the WCLL-TBM: 492 kW from nuclear heating and 231 kW from first wall heat flux.
- 200 s of ramp-down from full to zero plasma power.
- 1090s of dwell (no plasma power).

The most challenging normal operational state occurs at end-of-life conditions due to tube plugging and fouling expected on the internal and external surfaces of the heat exchanger tubes.

The pulsed regime also poses an additional burden to the components along the PL due to the fluctuating temperatures. The HT-0001 electrical heater is installed to partially counteract these variations keeping the coolant at TBM inlet at 295 °C. Although, due to the absence of plasma heating, the outlet coolant temperature decreases from 328 °C to 295 °C, thus affecting the operations of the HX-0001 economizer (the coolant bypasses the component).

Fig. 5 shows the evolution of the total pressure during two pulses. The code used for the analysis is RELAP5/Mod3.3. For the WCS, the adopted nodalization was the updated version of the input deck already employed in previous studies [7,8]. Referring to WL, the associated thermal-hydraulic model was created from data reported in [5,9]. The calculation starts with a flat-top phase (white), followed by ramp-down (blue), dwell (red), and ramp-up phases (green). The pulsed regime adopted by the ITER machine leads to an oscillating total pressure in the primary loop. During the dwell phase the coolant after the TBM shrinks due to its temperature decrease (Fig. 6) leading to a fast decrease in the pressurizer water level, and so to an abrupt fall of the pressure in the loop. The pressure control system counteracts this event by energizing the electrical heater installed inside the pressurizer, but about 15 min are required to restore the pressure at 15.5 MPa.

Then, the opposite problem occurs during the ramp-up and the flat-top phase. The coolant at TBM outlet heats up and expands leading to a

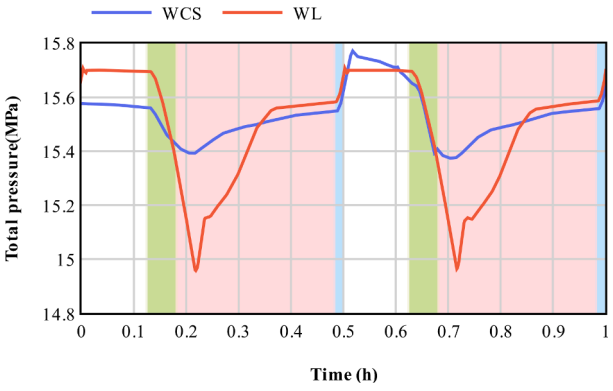

Fig. 5. Primary loop – total pressure.

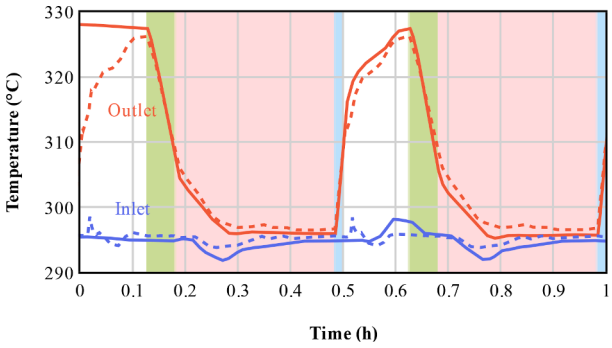

Fig. 6. TBM inlet and outlet temperature. WCS: straight lines: WL: dashed lines.

level increase in the pressurizer, and so to an abrupt pressure rise. In this case, the pressurizer spray system is activated to keep the pressure under control.

The complex behavior of the ITER WCLL-WCS is well captured by the ENEA WL facility. The total pressure in the primary loop (Fig. 5) oscillates due to the pulsed regime of the ITER machine, but WL present a more drastic pressure reduction due to the slightly longer pipeline at the outlet of the TBM. When the pressure increases during the ramp-up phase WL presents a different behavior due to the diverse simulation approach adopted for the control valve installed in the spray line. In WL, it is simulated with a RELAP5 valve component, opening at 15.7 MPa. Instead, in the WCS input deck, the component is modelled with a time-dependent junction whose imposed mass flow is proportional to the pressure deviation within the pressurizer, with a linear trend going from 15.7 to 16.0 MPa. For this reason, the WCS pressure peak is slightly higher than for WL.

The temperature evolution at the TBM inlet and outlet is shown in Fig. 6. Again, the difference shown in the first flat-top phase (0 – 0.12 h) derives from the simulation approach adopted: in WCS this flat-top derives from a long steady-state at full plasma power, while in WL it comes from a precedent pulse.

Other key temperatures in the loop are in good agreement, with a maximum difference of 4 °C shown at the outlet of the HX-1 shell (Fig. 7). A good agreement is also found for the secondary loop with maximum differences of 0.02 MPa and 1 °C (Figs. 8 and 9).

An overview of the exchanged powers by the TBM, the HT-0001 electrical heater, and the HX-0002 and HX-0003 heat exchangers is shown in Fig. 10. The differences in the first flat-top phase are again due to the different simulation approach adopted for this phase. The power to be provided by the HT-0001 electrical heater during the dwell phase is simulated following two different approaches in WCS and WL, but this does not influence the numerical outcomes. The power exchanged by HX-0003 between SL and the final heat sink is slightly lower in WL because of the higher heat losses toward the environment given by the different insulation material adopted for WL [5].

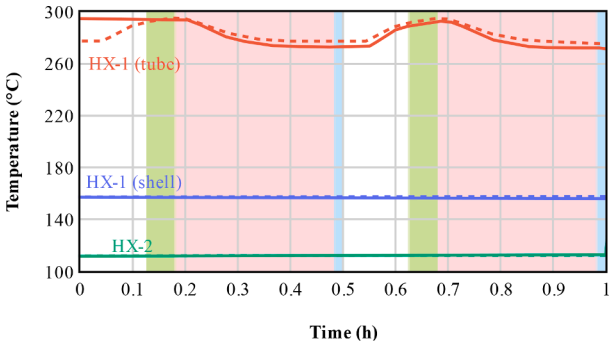

Fig. 7. HX-1 and HX-2 outlet temperature (primary loop).

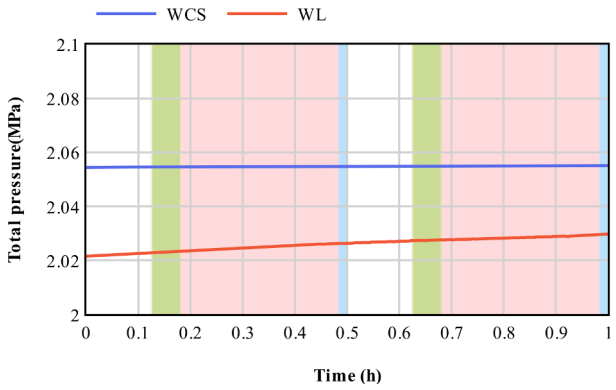

Fig. 8. Secondary loop – total pressure.

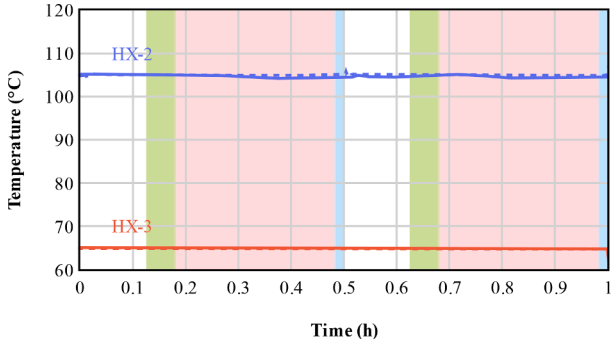

Fig. 9. HX-2 and HX-3 outlet temperature (secondary loop). WCS: straight lines: WL: dashed lines.

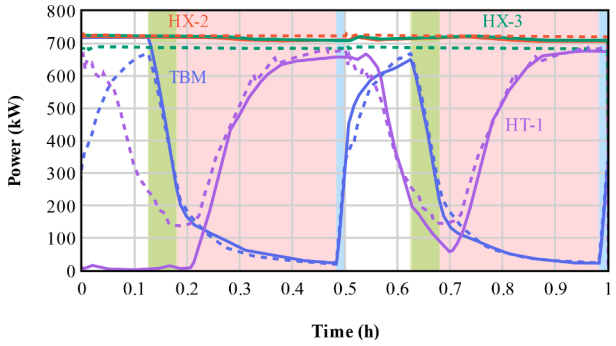

Fig. 10. Exchanged power by TBM, HX-2, HX-3, and HT-1. WCS: straight lines: WL: dashed lines.

6. Secondary loop loss of flow accident analysis

The secondary loop loss of flow accident is one of the most challenging transients for the pressure relief tank since the absence of leakages ensures the maximization of the dischargeable enthalpy in its volume. The severity of the accident is not high enough to require the activation of the fast plasma shutdown system, and the consequences to other components should not be so severe (e.g. risk of first wall melting) to trigger any mitigative action. Investigating this category of accidents is of primary importance also for EU-DEMO fusion reactor, as discussed in [10,11]

The accident was assumed to occur at the very beginning of the flat-top phase. The detection of the failure triggers the deactivation of the HT-0001 electrical heater, the deactivation of the pressurizer spray system (secondary loop), and the execution of next pulses. The flow rate in the primary loop is kept at 3.74 kg/s to remove the decay heat

produced in the TBM (1 % of total pulse power, i.e. about 7.23 kW). The evolution of the system for the first 24 h following the accident is analyzed being the most relevant part of the transient.

The comparison between WCLL-WCS and WL facility shows more relevant differences than that of the normal operational state. In terms of total pressure in the primary circuit (Fig. 11), the flat-top phase (in red) does not show any appreciable difference with a normal pulse. After the termination of the pulse the pressure decreases due to the shrinking of the coolant, and the electrical heater in the pressurizer is energized to restore the pressure value.

Then, 28 min after the termination of the pulse, too low coolant temperatures at TBM inlet are detected. To keep inlet temperature above the PbLi solidification point (>271 °C, Fig. 12) the HT-0001 electrical heater is reactivated. The heat provided leads to a swelling of the primary coolant causing a small increment of the loop pressure, but after 1 h from the failure the primary circuit finds a new equilibrium state.

Instead, the secondary loop presents a more complex behavior. After the pump trip, the average temperature and the pressure increase due to the heat coming from the primary loop (Figs. 13 and 14). The PORV opens when the pressure reaches 2.2 MPa and a small fraction of the secondary loop inventory is released inside the relief tank. This discharge, the absence of heat coming from the primary loop, and the heat losses toward the outer environment are sufficient to keep the pressure under control.

Nonetheless, when the HT-0001 electrical heater is re-activated, the secondary loop starts to receive about 200 kW. From here on, the differences in the layout of the secondary loop start to play a role (Figs. 15 and 16): in WL the heat exchanged through HX-0002 and HX-0003 presents an oscillating, but controlled, behavior, while in the WCLL-WCS a chaotic heat transfer occurs.

In WL a small, yet sufficient, natural circulation is established. This small flow rate is enough to transfer the incoming heat toward the final heat sink. Instead, in the WCLL-WCS, no natural circulation is established. This is due to the geometrical arrangement of the circuit, with long pipelines at high elevations that inhibit the natural circulation (see Fig. 1). Therefore, the incoming heat is released discharging steam from the pressurizer to the relief tank (Fig. 17). The water in the HX-0002 shell begins a process of evaporation and condensation leading to spikes in the system pressure that cause the opening of the PORV. The pressurizer inventory (400 kg) is released inside the relief tank in about 20 h, then the pressure starts to follow a decreasing trend due to small coolant inventory left in the circuit (less than 50%).

As the coolant level in the secondary loop pressurizer decreases, the level, pressure, and temperature in the relief tank increase (Fig. 18). A sensitivity study has been performed to assess the optimal water level in the relief tank at the beginning of the transient to avoid the opening of the rupture disk. Indeed, given the component volume, increasing the initial liquid content enhances the pressure-suppression function, but reduces the available expansion volume. The sensitivity study was

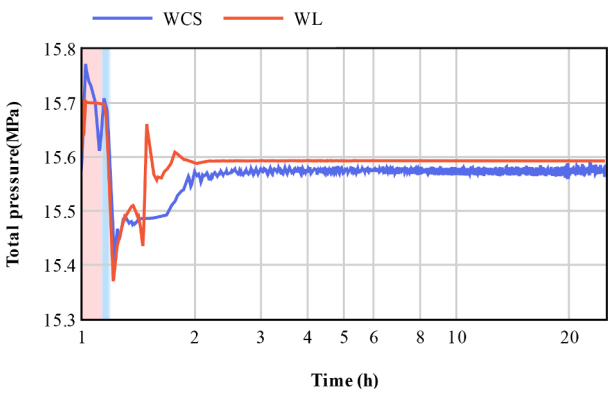

Fig. 11. Primary loop - total pressure.

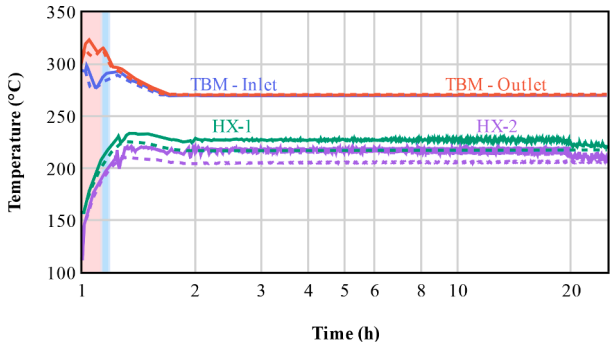

Fig. 12. TBM inlet & outlet, HX-1 outlet and HX-2 outlet temperatures (primary loop). WCS: straight lines: WL: dashed lines.

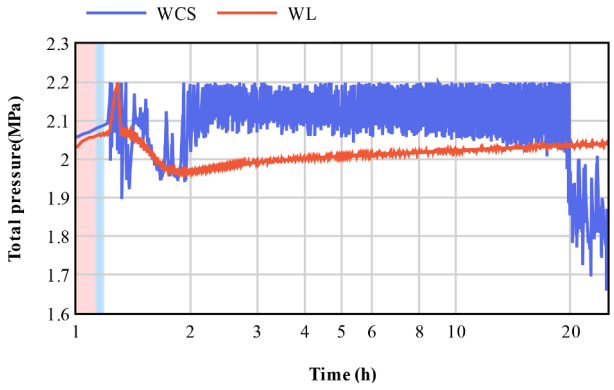

Fig. 13. Secondary loop - total pressure.

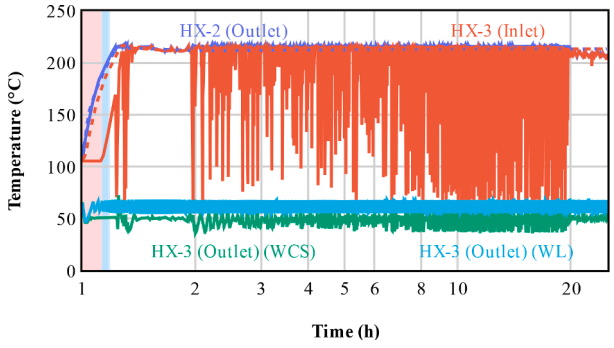

Fig. 14. HX-2 outlet, and HX-3 inlet & outlet temperatures. WCS: straight lines: WL: dashed lines except when for “HX-3 (Outlet)”.

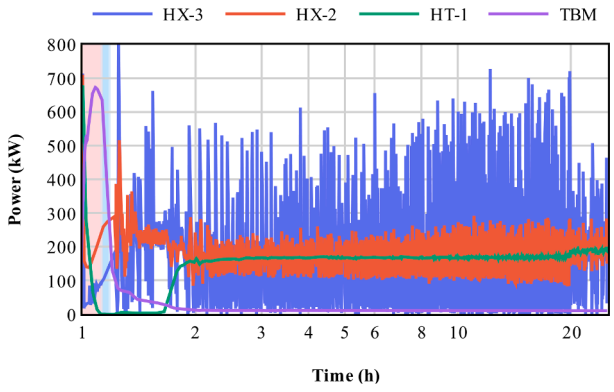

Fig. 15. TBM, HX-2, HX-3, and TBM exchanged power (WCS).

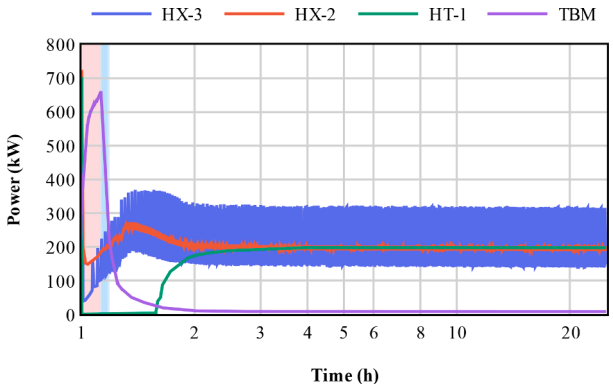

Fig. 16. TBM, HX-2, HX-3, and TBM exchanged power (WL).

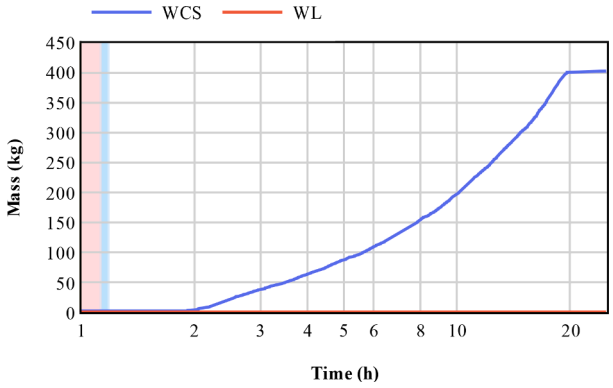

Fig. 17. Discharged mass in relief tank.

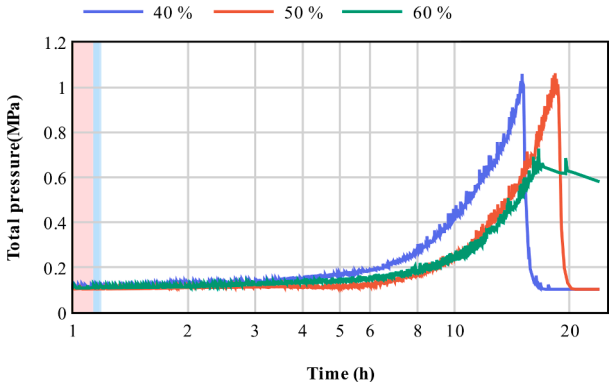

Fig. 18. Relief tank – total pressure.

aimed at understanding which one is the most important aspect to manage the overpressure transient occurring in the secondary loop. The study showed the possibility to avoid the opening of the rupture disk at 1 MPa (gauge) adopting an initial level equal to 60 % of the relief tank height.

7. Conclusions

The present paper showed a comparison between the ITER WCLL-WCS system and the ENEA WL facility. The WL facility is meant to be a thermal-hydraulic replica of the WCLL-WCS to test mock-ups, components, and operative procedures. For this reason, the ENEA WL facility should adopt the same WCLL-WCS components and mimic its layout.

An initial geometrical comparison was performed to assess the consistency of the WL and WCLL-WCS designs. WL showed good agreement for the component's barycenter position, but a different pipeline length. The primary loop was found to be about 23 m shorter, and local differences in the surrounding of the TBM were also highlighted. Instead, the secondary loop resulted 48 m shorter (50 % in relative terms) than the WCLL-WCS one. Differences were also shown for the height span of the heat exchangers, and on the pipeline position.

Then, thermal-hydraulic studies with the RELAP5/Mod3.3 code were done to investigate the behavior of the WCLL-WCS and the capabilities of WL. The first comparison was done considering the normal operational state at end of life. The two systems presented a comparable behavior, with minor discrepancies given by the different approaches adopted by the authors to simulate the circuits (user's effect).

The following thermal-hydraulic analysis focused on the behavior of the two facilities affected by a loss of flow accident in the secondary loop. In this case, the geometrical discrepancies of the secondary loop had a greater influence on circuit performances, leading to different accidental evolutions for the WCS and WL.

These studies highlighted two aspects that could be considered to further enhance the WCLL-WCS design:

- A natural circulation in the secondary loop could be established adopting a more compact layout with less ups and downs.
- The initial level in the pressure relief tank may be tuned to control the integrity of its safety devices (rupture disk) during off-normal conditions.

However, it must be noted that, after the conclusion of the current work, a revision of the ITER WCLL WCS layout within the TCWS vault was performed. Thus, the comparative analysis reported in this paper should be repeated considering this new system arrangement. For this, the described comparative method must be considered the main outcome of the presented activity, to be performed at each new design iteration.

CRediT authorship contribution statement

B. Gonfiotti: Conceptualization, Data curation, Formal analysis, Investigation, Methodology, Writing – original draft, Writing – review & editing, Visualization. **C. Ciurluini:** Conceptualization, Formal analysis, Investigation, Methodology, Writing – original draft, Writing – review & editing, Visualization. **F. Giannetti:** Conceptualization, Methodology, Resources, Software, Supervision, Validation, Writing – review & editing. **P. Arena:** Conceptualization, Methodology, Supervision, Validation, Visualization. **A. Del Nevo:** Conceptualization, Methodology, Project administration, Resources, Software, Supervision, Validation, Visualization.

Declaration of competing interest

The authors declare that they have no known competing financial interests or personal relationships that could have appeared to influence the work reported in this paper.

Data availability

The data that has been used is confidential.

Acknowledgments

This work has been carried out within the framework of the EUROfusion Consortium, funded by the European Union via the Euratom Research and Training Programme (Grant Agreement No 101052200 — EUROfusion). Views and opinions expressed are however those of the author(s) only and do not necessarily reflect those of the European Union or the European Commission. Neither the European Union nor the

European Commission can be held responsible for them.

References

[1] L.V. Boccaccini, F. Arbeiter, P. Arena, J. Aubert, L. Bühler, I. Cristescu, A. Del Nevo, M. Eboli, L. Forest, C. Harrington, F. Hernandez, R. Knitter, H. Neuberger, D. Rapisarda, P. Sardain, G.A. Spagnuolo, M. Utili, L. Vala, A. Venturini, P. Vladimirov, G. Zhou, Status of maturation of critical technologies and systems design: breeding blanket, Fusion Eng. Des. 179 (2022) 113116, https://doi.org/10.1016/J.FUSENGDES.2022.113116.

[2] A. Del Nevo, P. Arena, G. Caruso, P. Chiovaro, P.A. Di Maio, M. Eboli, F. Edemetti, N. Forgione, R. Forte, A. Froio, F. Giannetti, G. Di Gironimo, K. Jiang, S. Liu, F. Moro, R. Mozzillo, L. Savoldi, A. Tarallo, M. Tarantino, A. Tassone, M. Utili, R. Villari, R. Zanino, E. Martelli, Recent progress in developing a feasible and integrated conceptual design of the WCLL BB in EUROfusion project, Fusion Eng. Des. 146 (2019) 1805–1809, https://doi.org/10.1016/J.FUSENGDES.2019.03.040.

[3] F.A. Hernández, P. Pereslavtsev, G. Zhou, Q. Kang, S. D'Amico, H. Neuberger, L. V. Boccaccini, B. Kiss, G. Nádasi, L. Maqueda, I. Cristescu, I. Moscato, I. Ricapito, F. Cismondi, Consolidated design of the HCPB breeding blanket for the pre-conceptual design phase of the EU DEMO and harmonization with the ITER HCPB TBM program, Fusion Eng. Des. 157 (2020) 111614, https://doi.org/10.1016/J.FUSENGDES.2020.111614.

[4] I. Ricapito, F. Cismondi, G. Federici, Y. Poitevin, M. Zmitko, European TBM programme: first elements of RoX and technical performance assessment for DEMO breeding blankets, Fusion Eng. Des. 156 (2020) 111584, https://doi.org/10.1016/J.FUSENGDES.2020.111584.

[5] P. Arena, N. Badodi, A. Del Nevo, M. Eboli, B. Gonfiotti, D. Jaramillo Sierra, Design of the ENEA water loop facility in support of the design of the DEMO water cooled lead lithium breeding blanket, in: International Symposium on Fusion Nuclear Technology 15 (ISFNT-15), Las Palmas De Gran Granaria, 2023.

[6] A. Tincani, P. Arena, M. Bruzzone, I. Catanzaro, C. Ciurluini, A. Del Nevo, P.A. Di Maio, R. Forte, F. Giannetti, S. Lorenzi, E. Martelli, C. Moreno, R. Mozzillo, C. Ortiz, F. Paoletti, V. Pierantoni, I. Ricapito, G.A. Spagnuolo, A. Tarallo, C. Tripodo, A. Cammi, M. Utili, K. Voukelatou, E. Walcz, B. Lesko, J. Korzeniowska, P. Chiovaro, V. Narcisi, Conceptual design of the main ancillary systems of the ITER water cooled lithium lead test blanket system, Fusion Eng. Des. 167 (2021) 112345, https://doi.org/10.1016/J.FUSENGDES.2021.112345.

[7] C. Ciurluini, F. Giannetti, A. Tincani, A. Del Nevo, G. Caruso, I. Ricapito, F. Cismondi, Thermal-hydraulic modeling and analysis of the water cooling system for the ITER test blanket module, Fusion Eng. Des. 158 (2020) 111709, https://doi.org/10.1016/J.FUSENGDES.2020.111709.

[8] C. Ciurluini, V. Narcisi, A. Tincani, C.O. Ferrer, F. Giannetti, Conceptual design overview of the ITER WCLL water cooling system and supporting thermal-hydraulic analysis, Fusion Eng. Des. 171 (2021) 112598, https://doi.org/10.1016/J.FUSENGDES.2021.112598.

[9] A. Del Nevo, P. Arena, M. Eboli, P. Lorusso, A. Tincani, N. Badodi, A. Cammi, F. Giannetti, C. Ciurlini, N. Forgione, others, The design of water loop facility for supporting the water coolant lithium lead breeding blanket technology and safety, Energies 16 (23) (2023) 7746, https://doi.org/10.3390/en16237746.

[10] C. Ciurluini, F. Giannetti, E. Martelli, A. Del Nevo, L. Barucca, G. Caruso, Analysis of the thermal-hydraulic behavior of the EU-DEMO WCLL breeding blanket cooling systems during a loss of flow accident, Fusion Eng. Des. 164 (2021), https://doi.org/10.1016/j.fusengdes.2020.112206.

[11] C. Ciurluini, F. Giannetti, A. Del Nevo, G. Caruso, Study of the EU-DEMO WCLL breeding blanket primary cooling circuits thermal-hydraulic performances during transients belonging to LOFA category, Energies 14 (2021), https://doi.org/10.3390/en14061541.